A Macroscopic Fundamental Diagram for Airplane Traffic: Empirical Findings

Victor L. Knoop, Joost Ellerbroek, Mark ter Heide, and Serge Hoogendoorn

Author manuscript of Transportation Research Record: Journal of the Transportation Research Board Volume: 2679 Issue Number: 2

Abstract

For car traffic it was found that a more crowded area leads to a lower speed and a lower arrival rate. The relation between crowdedness and speed (or arrival rate) can be expressed in a network fundamental diagram, or macroscopic fundamental diagram (MFD). Similar concepts have been shown for pedestrian and train traffic. In this paper, we extend the concept to 3 spatial dimensions (3D). While simulations have explored some concepts, we present for the first time empirical results of the relation between the crowdedness in the air and the performance of the "network". We base our results on several months of data of planes around Amsterdam Schiphol Airport. Similar to car traffic, we observe a reduction in speeds as the number of airplanes in the area increases. However, even at the highest observed densities, we do not see a reduction in flows. This is due to active and intensive management (based on departure/landing possibilities), comparable to perimeter control in traffic, as well as a minimum airplane speed. This paper introduces an interesting concept of applying an MFD to 3D spaces. We also show to what extent the performance reduction is due to speed reduction and to what extent it is due to less efficient routes. The MFD concept can eventually be used to also manage 3D air spaces for applications with less strict microscopic air traffic management than the current management around airports.

Key words: Traffic operations, traffic flow theory, fundamental diagram, macroscopic fundamental diagram, MFD, NFD

1 Introduction

Air traffic as mode of transportation has been rising rapidly over the past decades (for example (Statistica, 2022)), which has increased the number of planes. Despite the many differences, it is interesting to compare aviation to car traffic. Due to the large number of cars present, car traffic management often uses modelling and control approaches which describe traffic on an aggregated level. This means that there is no need to describe each individual vehicle. For car traffic, models and control are developed on different levels of description. There is a microscopic level, which models and controls individual cars. There is also an aggregated level, a macroscopic level or even a network level, in which traffic is described at a road level or a network level, without considering individual vehicles. This is in line with for instance fluid dynamics where not all individual particles are being modelled, but predictions are made on the level of a flow. At this level, models and control are made using the properties of the stream. Such a higher level of description becomes more relevant if the number of particles increases. Since a continued rise in the numbers of planes is expected in air traffic, it is worthwhile to investigate the properties of the stream also for air traffic, using models derived from car traffic research. If applicable, these can form the basis for modelling and control at higher aggregate levels.

In the past decade and a half, area based traffic management for car traffic has received an increasing amount of scientific attention. This boost of attention started with the publication by Daganzo (2) arguing there should be a relationship between the number of cars and their average speed *on a zone level* (i.e., exceeding the level of a single road; one can think of a city center). Moreover, Daganzo posed that due to a decreasing speed of the cars with increasing densities in the zone, the flow (also called production for a zone) should have a maximum point at some density. The relation between average speed and density in a zone has since then been referred to as Macroscopic Fundamental

Diagram (which we will be using in this paper, abbreviated MFD), or (equivalent) Network Fundamental Diagram. For road traffic the flow-density relationship presented in the MFD is typically non-linear, where flow increases with density up until a certain critical value. Increasing density beyond this critical value leads to a reduction in flow, and an increase in overall travel travel time. Since then, many papers have started working on control schemes which keep the density in a zone below this critical density (e.g., (Keyvan-Ekbatani et al., 2012)). Interestingly, (Daganzo, 2007a) already mentioned that the concept of reduced speed with increasing density of particles (of whatever kind) would not only hold for road traffic, but many other processes, even including "your desktop".

A significant part of Air Traffic Management (ATM) consists of air traffic controllers managing individual flights, to keep them at safe distance from each other. In current-day ATM, air traffic is also managed at a flow level (through a process called Air Traffic Flow Management, ATFM), which is meant to ensure that the capacity of airports (and to some extent airspace sectors) is not exceeded. The main regulation that ATFM can impose is a departure delay, which is why current ATM research is focusing on other approaches as well, to better accommodate the rise in air traffic. With the recent rising interest in urban aerial transportation, network-constrained air traffic is now also studied, for instance with models for local interactions like intersections (Doole et al., 2021), or organisation of the airspace using virtual tubes (Cummings and Mahmassani, 2023). Free-flowing intersection capacity is further investigated by (Aarts et al., 2023).

Recently, a couple of works have presented simulation to test whether large-scale traffic descriptions also work for air traffic, and, more specifically, whether an MFD can also be used for air transport to draw conclusions on capacity and throughput in a similar way to road transport. The first efforts by Cummings and Mahmassani (*7*) show that also in 3-dimensional (3D) air (drone) traffic, a relationship between flow and density would emerge on the area level. (Note in this paper we will adopt the convention to count only spatial dimensions; when including time, the same concept would be called 4-dimensional). Tereshchenko et al. (*8*) also shows MFDs for air traffic. This paper mentions effective distance covered: using great-circle (shortest-path) distance to represent non straight paths. The work by Haddad et al. (*9*) utilizes the concept of an MFD to apply perimeter control in 3D airspace.

In this paper we present an empirical verification of the Macroscopic Flow Diagram for conventional air traffic. First, the next section will give more background on the origin and the use of the MFD in car and air transportation. Key to note is that the papers discussing and exploiting an MFD for air traffic use (microscopic) simulations as basis, and this MFD has not been empirically verified.

For car traffic, validation of the MFD using empirical data from Yokohama (Geroliminis and Daganzo, 2008) has accelerated the use of the concept of the MFD, which has led to models on the zonal level and many control concepts. With the current work, we would like to address the absence of an empirical MFD for air traffic. We aim to show that the relationship between density and production holds in air traffic as well. This can form the basis for air traffic modelling on an aggregated level, which can ultimately be used in the design of new air traffic control concepts.

Air traffic with planes is fundamentally different from car traffic. Near airports, all planes need to land or depart from a limited number of runways. There is hence a very centralised hotspot rather than a central business district with some spatial extension. Secondly, near airports, air traffic is microscopically controlled in a centralised manner. Hence, inefficient traffic operations due to drivers that block intersections or so should not occur. Finally a major difference is that planes have a non-zero minimum speed (some margin above the stall speed) below which they cannot operate. Contrary to cars, planes cannot reduce their speed under a certain threshold to wait for other planes because they would simply fall to the ground. Options to delay planes are flying (a bit) slower or take a detour. This happens a lot at some airports.

To delay an (airborne) aircraft in case of congestion, air traffic controllers can make use of four different strategies: The simplest strategy is *linear holding*, which corresponds to a reduction in speed while maintaining the original track. As described above, this strategy is limited by the minimum operating speed of aircraft. The second strategy, often applied at the entry points to terminal airspace (initial approach fixes, IAF), is to put aircraft in a *holding stack*; a circular or oval pattern, that adds a fixed amount of delay for each full round in the stack. The third strategy, *tromboning*, is applied just before landing, where the flightpath of the aircraft is extended along the centerline of the runway. With the fourth strategy, *vectoring*, air traffic controllers delay an aircraft by deviating them from their original path by a fixed course change.

The application area of an MFD for airborne traffic will most likely lie in a low-altitude airspace with many drones, possibly flying autonomously following collision avoidance or priority rules. This is a different use of airspace than

the current air traffic near airports. We would hence not expect the same MFD to appear in this low-altitude drone traffic as we might find in conventional air traffic. The aim of this paper is to for the first time show empirical evidence of an MFD for 3D traffic. Therefore, in this paper we will answer two questions. The main question is: what does a macroscopic fundamental diagram for air traffic near an airport look like? A subquestion related to this is: how to best express the relevant variables for and MFD for air traffic, since the principles for delay (detour instead of slowing down) are fundamentally different?

The remainder of this paper is set up as follows. The next section first gives a more extensive scientific background on (empirical) MFDs and traffic control for both air traffic and MFD-related control for car traffic. Then, the "Methodology" section presents the methods we use to create the MFDs. The data we will be using is described in section "Data", followed by a section "Results" which presents the MFDs and their interpretation (and comparison to car MFDs). The final section presents the conclusions and potential applications.

2 Literature review

The main macroscopic variables in traffic engineering are flow (i.e., the amount of traffic passing by a point on the road in a unit of time), denstiy (i.e., the number of vehicles per unit of space) and average speed. The difficulty is that flow and density are measured along different dimensions (one along time and one along space), which makes it impossible to rightfully relate flow and density in the same observation span to each other. In 1965, Edie (Edie, 1965) presented his generalized definitions of traffic. He argued that flow, density and speed could be measured over an arbitrary area in space-time. These have been the cornerstone for traffic engineering since. He defined the following:

$$\text{Flow[veh/h]}q = \frac{\text{Total distance covered [veh km]}}{\text{Area in space x time [km h]}} \tag{1}$$

$$\text{Density [veh/km]}k = \frac{\text{Total time spent [veh h]}}{\text{Area in space x time [km h]}} \tag{2}$$

$$\text{Speed [kmh]}v = \frac{\text{Total distance covered [veh km]}}{\text{Total time spent [veh h]}} \tag{3}$$

The elegance of these equations is that they simplify to the intuitive relations for flow and density either applied to a period of time at single location (measuring flow) or a single moment in time over a road stretch (measuring density). A natural extension applied in MFD-related works is to define the "area in space time" as the product of the aggregation interval, times *the total road length* in the zone. For pedestrian traffic, a 2-dimensional (2D) process, flow is similarly defined with the area as 2D space. This yields a flow in pedestrians per meter per hour, which can be interpreted by how many pedestrians pass by in one unit of time over one meter of width of the road (typically perpendicular to the walking direction). The density is expressed in pedestrians per square meter. Extensions to 3D traffic, as well as our proposed extension for plane traffic, follow in the next section.

Air traffic at and around airports is typically managed by the control tower. This tower has a complete overview of the gates, taxi-ways and runways. The traffic is managed by air traffic controllers who are using visual and instrumental observations. The controlling system is based on flight progress strips. Such a strip contains individual flight information of the airplanes which are currently operating on the airport. The strips are categorized per operation status, for example: flights that have started up but have not started taxiing yet or flights that are in the taxi phase. These categories are designated to specific areas in the control tower. A specific air traffic controller is then responsible for a specific area. So air traffic is controlled on individual level. Without the clearance of air traffic control, airplanes at or near controlled airports are not allowed to move around. In general, a ground delay program can assist this and keep aircraft on the ground to limit airborne holding. (Administration, 2023)

As mentioned in the introduction, a couple of works have studied MFDs for 3-dimensional (drone) traffic, using simulation(Tereshchenko et al., 2020; Haddad et al., 2021; Cummings and Mahmassani, 2021). As far as the authors are aware, no empirical works have been published, and none studied the MFDs for conventional airplane traffic.

For car traffic, the first speed-density relationships for a network were mentioned and shown by simulation in Godfrey (*13*) and Mahmassani et al. (*14*). Then, a revival of the concept started, as mentioned, by the realisation that flow decreases when increasing density beyond a critical point (Daganzo, 2007b), with the first empirical results

presented in (Geroliminis and Daganzo, 2008). Since then, many papers have followed on control, which we discuss below. The original paper from (Geroliminis and Daganzo, 2008) used data from taxis in Yokohama.

Later works have for instance verified the concept using loop detector data (e.g., (Knoop and Hoogendoorn, 2013)) or using data of all Android phones (Knoop et al., 2018). This comes at a cost if not all vehicles are probed (Du et al., 2016). Later studies have proposed to combine different data sources (Ambühl and Menendez, 2016). The empirical validation of the concept of the MFD accumulated so far with the work of Loder et al. (*20*), showing the empirical MFD for more than 40 networks. Note that these empirical MFDs seldom show a properly "congested branch", i.e. a branch for which the total production decreases with a higher accumulation. This does happen quite often in simulations with extensive loading, or due to instabilities which cause some parts of the network to become unstable (see e.g., (Gayah and Daganzo, 2011; Hani Mahmassani and Zockaie, 2013)).

Also for other modes MFDs have been explored and presented. The most surprising might be the exploration of MFDs for train networks (Cuniasse et al., 2015). Note that this is a proper network-wide MFD, and the paper explicitly indicates the differences with car traffic. More relevant to air traffic might be the work exploring and explaining MFDs for pedestrian traffic (e.g., (Hoogendoorn et al., 2017)). The similarity with air traffic is that pedestrians can be considered as 'particles' that move in a continuous multi-dimensional space. For pedestrians, an MFD was found in empirics and a modelling form or explanation has been proposed. For further extensions of MFDs including modelling and multiple interacting classes we refer to the recent literature review by (Johari et al., 2021).

For car traffic, in the past decade various control schemes using the MFD were proposed. Knoop et al. (*26*) proposed to route cars based on the crowdedness (and speed) in the network; the original responsive routing can also be applied in a model predictive control framework (Hajiahmadi et al., 2013). This approach implicitly applies perimeter control, but at a section with multiple reservoirs. Perimeter control itself is pioneered by (Geroliminis et al., 2012) for a theoretical case and by (Keyvan-Ekbatani et al., 2012) for a realistic case with simulation. They both show that limiting the inflow to a zone can give large benefits in terms of total travel time. The aim in both cases is to not let the density exceed the critical density for a given zone. This has been further tuned, and extensions on this process still are subject of study (e.g., control delays, (Yuan et al., 2022)).

3 Methodology

To obtain an MFD for conventional air traffic, we extend the concepts of Edie (*11*). As argued by Cummings and Mahmassani (*7*), in principle Edie's definitions also apply to air traffic:

$$q = \frac{\text{Total distance covered [veh km]}}{\text{Area in 3D-space x time}[m^3 h]} \tag{4}$$

$$k = \frac{\text{Total time [veh h]}}{\text{Area in 3D-space x time}[m^3 h]} \tag{5}$$

Linear holding would reduce a plane's speed; the other mentioned delay strategies (vectoring, tromboning, and holding) involve path stretching. A better way of indicating the production of an airspace is the *effective distance covered*: the shortest path from the starting point of an aircraft to its destination. For airplanes we take the shortest path at a constant altitude. Since the earth is curved, the shortest path between two points is the so-called great circle path, with the matching great circle distance. For the distance of a single air plane, we hence define the production and density as follows:

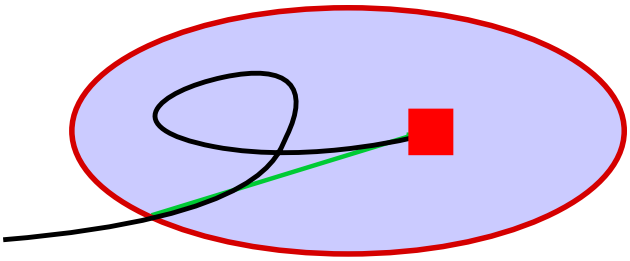

Figure 1: A considered area in space-time (blue shaded) and a hypothetical path of an airplane (black line) to an airport (red square). The green line denotes the effective distance.

$$
\begin{aligned}
P &= \frac{\text{Total effective distance covered [veh km]}}{\text{Area in 3D-space x time [m}^3\text{ h]}} \\
&= \frac{\sum_{\text{All airplanes}} \text{Effective distance covered [veh km]}}{\text{Area in 3D-space x time [m}^3\text{ h]}} \qquad (6) \\
k &= \frac{\text{Total time [veh h]}}{\text{Volume in 3D-space x time [m}^3\text{ h]}} \\
&= \frac{\sum_{\text{All airplanes}} \text{Flying time in area [veh h]}}{\text{Volume in 3D-space x time [m}^3\text{ h]}} \qquad (7)
\end{aligned}
$$

In this equation, only the effective distance is taken into account towards the production. The resulting effective speed is the quotient of this effective distance and the total time spent traversing this distance:

$$v = \frac{P}{k} = \frac{\text{Total effective distance covered [veh km]}}{\text{Total time spent[veh h]}} \qquad (8)$$

In this paper, we mix various disciplines with their own tradition of units. We will use the metric system to indicate flows (production), densities and speed, since they are easier to relate to each other than mixing miles and knots. For altitude indications, we stick to feet (and flight levels, which are 100 feet), to maintain well-rounded values for the altitudes.

To construct an MFD, we take all flight movements in an area around an airport between altitudes 5,500ft and 19,500ft. We aggregate all movements (i.e., sum all effective distances and times spent) over a period of 30 minutes.

We will construct the figure of the production versus the density. Since the situation of an empty air space means no density and no flow, the graph should start from the origin. Then a point cloud will show production. For car traffic, we know that the production will reach an optimum (Loder et al., 2019). In simulated conditions, the flow might even reduce with increasing density because of gridlocks occurring (e.g., (Daganzo et al., 2011; Gayah and Daganzo, 2011). In those cases, vehicles block each other in a circular way, leading ultimately to standstill of all vehicles. In practice, higher densities than the density matching the density for which the production is highest are seldomly reached.

The gradient of a line from the origin to a point indicates the effective speed of the planes during that period. We can also express this effective speed of the planes in the aggregation interval, and show its relationship with density. We expect this to more clearly show differences in speed.

The effective speed for an empty airspace will be called free speed, in analogy with traffic engineering. Note that this is not the speed of an individual airplane, but can be interpreted as the mean of the speed of all airplanes, and only considering the effective movements (see figure 1). We will quantify a free flow speed by finding the median speed of the low densities.

Now let's discuss efficiency. In the ideally effective world, planes would have no interference, and the effective speed would remain constant. We define efficiency as part of the production that is actually in the system compared to this ideal case:

$$\eta = \frac{P}{k v_{\text{free}}} \qquad (9)$$

We will analyze the loss of efficiency with increasing density. Note that, due to our definition, this can come from planes flying slower and/or planes taking a longer route. We will explicitly derive the origin of the loss of efficiency. That means, we will beside the effective path length also record the factual path length during each aggregation interval (see figure 1). The ratio of the two shows which part of the loss of production is due to the increase in path length, and hence the other part is due to the decrease in speed.

Let us note that speed for planes is more complex than speed for cars. The only relevant variable for car speed is the speed difference with the ground. For airplanes, its speed compared to the wind, the true airspeed (TAS). This is related to ground speed. The difference between the ground speed the true air speed is the wind speed. Moreover, an airplane takes the indicated airspeed (IAS) as reference. This is what the gauges indicate. This speed depends on the dynamic pressure of the plane, and hence depends, next to the true airspeed, on the air pressure and is hence related to the altitude. When descending under constant IAS, the air pressure increases, so the true air speed (and hence the ground speed) will reduce. As a rule of thumb, the following can be used $TAS = IAS +$ flight level$/2$, in which units of knots and are used; flight level is the altitude in 100 feet. Hence 200 knots IAS at FL250 (i.e., 25,000 feet; 370 km/h or 230 mph) equals (approximately) the same TAS as 325 (600 km/h or 375 mph) knots at ground level.

To illustrate (potentially small) changes in effective speed even more, we will also show how differences between effective speed and free speed relate to the density. We expect that this difference will increase with increasing density.

4 Data

We will analyse the data for Amsterdam International Airport Schiphol (AMS). Schiphol is one of the busiest airports in Europe with around 72 million passengers per year, and approching 500,000 airplane movements (pre-covid numbers; (Schiphol Amsterdam airport, 2022)). It is located in a almost level area, and there is no interference from geography with the flights. Due to the amount of data, we make a selection in months. We will be using all data from April and August 2019 (regular and holiday season, both pre-COVID19), and from April and August 2020 (low flight numbers due to COVID19, with the low due to Covid in April 2020). Typically, there are quiet periods during the night and more busy periods during the day with typical peaks. Figure 2 shows the number of planes in the considered area as function of the time of day. It shows that in the aggregation interval there are 60+ planes which is sufficient to get a reliable estimate for flows and density. We also show the density of the planes based on these numbers. Note in this figure also the large effects of the COVID pandemic, with April 2020 having 87% fewer flights than April 2019.

The airspace near Schiphol is divided in three main categories. From small to larger these are the Controlled Traffic Zone (CTR), Terminal Manouvering Area (TMA), and Control Area (CTA). The CTR is the zone controlled by the air traffic control tower on the airport. In this airspace the initial departure and final approach take place. Air traffic controllers control this zone with direct visual observations and instrumental observations. The TMA is controlled only by instrumental observations, with air traffic controllers sitting in a control room. The TMA holds the departure and arrival routes. Holding stacks are typically placed at the edge of the TMA, alongside a limited number of Inital Approach Fixes: fixed entrypoints into the TMA. CTA airspace is situated at altitudes above the TMA, and contains flights in cruise, and flights transitioning to and from cruise flight.

We will be using the CTA since it includes the flights approaching and departing from Schiphol airport. To include sufficient area, we include the 5 Dutch CTAs combined, see figure 3. We will be using only the data between FL055 and FL195 (i.e., 5,500 and 19,500 foot) to exclude airplanes crossing this area and not interacting with the manouvering planes. Finally, note that the airspace consists not only of airplanes in- and outbound from Schiphol but also of airplanes heading to or from other airports relatively close by. Air traffic of airports Eindhoven, Rotterdam, and Düsseldorf also pass through the considered area, and will hence also affect air traffic near Schiphol airport. Since the airplanes are within the airspace they contribute to the density and flow of considered area are part of the analysis. On average, these flight account for 17% of the flights in the considered airspace Ministerie van Infrastructuur en Milieu; Dutch Ministry of Infrastructure and Enviroment (2012).

The surface area of the considered area measures 42,807 km^2. The height is 19,500 ft - 5,500 ft = 14,000 ft = 4.28 km. The total volume hence is 42,807 * 4.28 = 182,667 km^3.

For this research we will be using data from the Automatic Dependent Surveillance-Broadcast (ADS-B). The data are recorded by a receiver at the top of the aerospace faculty building of the Delft University of Technology. Range is limited to the line-of-sight due to the curvature of the earth. The range is larger than the range required for this

research and hence does not form a limiting factor. These data contain for each plane: ICAO aircraft address (unique ID), Latitude, Longitude, Altitude, Ground Speed, Track (degrees), and Rate of Climb. These data are periodically broadcast by every plane equipped with an ADS-B transponder. Each message is time-stamped upon reception.

We use the data to find the point and time of entry into the CTA at the desired altitude, and the point and time of entry out of the CTA at the desired altitude. We do so for every flight. An example with two airplanes is shown in figure 3. Note that there are several starts possible to be included in the considered data: while being at the right altitude once it crosses the boundary (the orange/purple line) or the while it is inside the CTA once it reaches the right altitude (green/red) line. Typically, the included parts of a flight are (1) a flight from the boundary to the airport or vice versa, (2) a flight from the boundary to the boundary, or (3) A flight from the boundary to a point in the area (or vice versa), or from the airport to a point in the area (or vice versa); this happens if the aggregation interval starts or ends in the flight though CTA.

5 Results and discussion

First, let us discuss the MFD presented in figure 4. Figure 4(a) and Figure 4(b) present the same data in different ways. Figure 4(a) shows a scatter plot of the density versus production. It also shows (in red) a line with constant slope (free flow speed, see below), and a fit of the data (in purple, see also below). Because the scatter plot does not clearly show the width of the point cloud, figure 4(b) shows the same data, where we also express the data by a median line and a 17 and 82 percentile value in blue. These values represent the inclusion of the mean and plus or minus 1 standard deviation in case of a normal distribution.

The figures show an observed density range between 0 and approximately 0.0002 airplane per cubic km. Let's first consider the range of the plot. The minimum separation to any other plane is 5 nautical miles in each direction (9.62 km) in the horizontal plane, and 1,000 ft up and 1,000 ft down (2 x 0.305 km). This means a plane would need a disk for itself. The volume of this disk is $\pi(9.62)^2 \times 2 \times 0.305 = 177 km^3$. If we could pack them without voids, a maximum density could be achieved of $1/177 = 0.0056$ planes/km^3. Since disks cannot be placed next to each other without voids, there is a packing inefficiency (when arranging the disks optimally in a hexagonal packing). Geometrically it can be derived that then only $(\pi\sqrt{(}3)/6 \approx 91\%$ of the space can be used. The maximum density then becomes $1/177 \times 0.91 = 0.0051$ planes/km^3. Note that this theoretical maximum can only be achieved if either all airplanes are stationary, or when all airplanes are flying at the same speed, in the same direction.

The found range to 0.0002 planes/km^3 is indeed well below the theoretical maximum density if all airplanes were at their minimum separation.

As hypothesised we see that flow is increasing with density up to the highest densities reached. We do see, however, that the gradient of the relationship between effective production and density is decreasing with increasing density. This indicates that as densities go up, effective speeds reduce. The width of the distribution is notably smaller than the increase, indicating that the increase is significant. Moreover, the comparison of the constant speed line and the bounds of the MFD show that the reduction of effective speed is also beyond the natural fluctuations.

The speeds are also shown in figure 5 with the same line styles and colors as figure 4. In very low densities, we see a high variability in speeds. This is due to the fact that these densities are observed in situations where only a part of the trajectory of a single flight falls into the area of interest. For instance, a plane takes of at 5.29 am and no flights have been recorded earlier. Then, only the first minute of that flight falls into the aggregation area. The effect is similar for take-offs or for planes crossing the CTA. All in all, the aggregation areas with very low density are not very reliable. We therefore set the free flow speed as the mean of the average speed of percentiles 3-8. We found the percentiles by checking the lowest percentiles where the free flow speed becomes constant. We find a free flow speed of 442 km/h (239 knots). Note that this is close to the CTA procedural maximum speed of 250 knots.

The red line in figure 4 indicates the free flow speed. It is clear that the effective speed of the airplanes reduces with density. We hence also show a fit of the MFD according to a linearly deceasing speed. Fitting a fundamental diagram is not trivial, and a good approach is fixing some degrees of freedom (Knoop and Daamen, 2017). The data is relatively scattered, hence we choose a fit with a low number of parameters to be fitted. In fact, we choose a second-order fit (parabola shape, or in traffic engineering terms a Greenshields fundamental diagram), for which we fix the free-flow speed to the found value of 442 km/h. Moreover, in line with traffic engineering principles that no density yields no flow, we require the parabola to fit through (0,0). Now, two degrees of freedom have been set, which reduces

the freedom in the fit to 1. The resulting parabola shape fit is shown in figure 4 as well, and follows the point cloud nicely. The theoretical jam density found is 7.8E-4 planes/km^3, and according to the model fit the highest flow would be found at 3.9E-4 planes/km^3. That still is almost an order of magnitude below the maximum packing density of planes based on their minimum separation. Figure 6 shows the routes taken and shows that a large part of the space is unused. This is a 2D representation and indeed even in the used paths not the full altitude range is used either. This explains the lower density ranges.

In car traffic, the MFD was first hypothesised to strongly decrease for higher densities. Whereas that theoretically might indeed be the case, it turns out that for empirical MFDs, the congested branch is not complete and the production curve stops just beyond the critical density. This has been shown for most of the empirically found MFDs (Knoop and Hoogendoorn, 2013; Loder et al., 2019). Also for air traffic, as expected, the MFD does not reach the top of the production, because air traffic is better planned and airplanes do not reduce their speed to standstill to queue. For some airports, such as London Heathrow, holding stacks are more common, and one might see a larger reduction in flow.

We consider efficiency in terms of the directness of the paths flown. Similar to the free-flow speed, we also define a free-flow efficiency, which shows the loss of efficiency also at low speeds. This is based on the ratio of the path lengths for the 3rd to 8th percentile density range. This free-flow efficiency is slightly above 80%. Figure 7 shows the efficiency as function of the density. We also include a line what would have been the efficiency if only speeds changed. This line is based on the Greenshields fundamental diagram, as fitted earlier in figure 4. The figure shows that the flow reduction is much stronger than the reduction in efficiency, meaning that the reduction in production is largely due to a reduction in speed. That is also visible by comparing figure 7 with figure 5a. The joint effect of reduction of speed and reduction of efficiency should cause the effect indicated by the magenta line. The reduction in free speed is much larger than the reduction of efficiency.

Figure 6 shows the routes planes take for a busy hour. It shows that the plane trajectories spiral out, but as expected, mainly follow predefined paths instead of a uniform distribution over the available airspace. It is visible, for instance at the bottom, that some planes cross the CTA and are not departing or landing at Schiphol. This is shown in another way that airplanes are not too much in each others path, but they are mainly following the same streams.

6 Conclusions and potential applications

This research has presented a method to produce a meaningful Macroscopic Fundamental Diagram for air traffic. A crisp MFD occurs. We have seen that with higher densities of airplanes the effective speed reduces. Yet, the flow is still increasing and we do not reach (let alone exceed) densities for which maximum flow occurs, as observed in road traffic. The computed critical density for which that would happen, extrapolating a fitted Greenshields fundamental diagram, is 2-3 times the highest densities currently achieved.

The fact that these densities are not reached could be explained by various factors. Indeed, the area chosen is quite large compared to the area used for flying. A smaller area closer to the airport would possibly yield denser traffic, but would also be even more stuctured and tightly controlled, as it would mainly involve airplanes in their final approach, or initial departure to and from the runway. Also, high-density situations which would result in low speeds and potentially a decrease in flow are actively avoided by the air traffic controller. The fact that airplanes cannot fly at very low speeds, as well as the comfort and efficiency of the airport play both a role here. Through for instance ATFM regulations (resulting in ground holding), but also through holding stacks a form of perimeter control is applied: Air Traffic Control does not allow more planes into the controlled airspace than the airport and airspace can handle.

The MFD does show to which extent the speed reduces with higher loads. There can be various reasons for this speed reduction. It should not be used as way of comparatively assessing the airport or the air traffic control. Having said so, it would be interesting to see how they compare for various airports and find to which extent the shape (qualitatively and quantitatively) differs for different airports. Also the underlying causes for these differences could help to understand the effectiveness of airports, and potentially thereby improving their efficiency.

The current research has established an MFD based on empirical data from several months. It aggregated the data of all conditions. Indeed, several factors can influence this relationship, and given the empirical approach will have done so. Some factors to mention are as follows: severe weather limits the capacity of airports and runways, strong winds change ground speed as compared to air speed, and weather cells may cause the usable area of a sector to be reduced, or even cause flights to be rerouted to alternate airports. Also in general this study investigates CTA traffic

in isolation, even though in practice it has to be acknowledged that e.g., runways as limiting resources, and spacing constraints that vary with aircraft performance (specified in wake turbulence categories), pose constraints on traffic flow in the terminal area which in turn also affect traffic in the CTA. A follow-on study should further investigate the effect of these individual constraints, either data driven by separating the data in various classes or by simulation.

The MFD could potentially also be applied for determining the level of control for air spaces. We propose ideas here which are not reasonable to apply in current air transport, but might be - in future times - applicable for drone traffic. With a large number of aircraft, decentralized control probably takes over individual conflict resolution. Air traffic control could be in the background up to the density that efficiency decreases with more than X%; for higher densities, air traffic management would then start intervening. An option for this intervention could be a form of perimeter control where aircraft should stay out of a zone for as long as density is too high.

7 Statement of contribution

V.L. Knoop is main author of the manuscript. Analyses and concepts were initiated by Victor Knoop and performed by Victor Knoop and Mark ter Heide. Joost Ellerbroek provided contributions from the domain of airport and airplane operations, and Serge Hoogendoorn from the overall field of transportation. Minor textual changes were incorporated after a proofread of ChatGPT. All authors have read and reviewed the manuscript.

8 Conflict of interest

There are no conflicts of interest.

References

Statistica, 2022, https://www.statista.com/statistics/564717/airline-industry-passenger-traffic-globally/.

Daganzo, C., Corrigendum to "Urban gridlock: Macroscopic modeling and mitigation approaches" [Transportation Research Part B 41 (2007) 49-62]. *Transportation Research Part B: Methodological*, Vol. 41, No. 3, 2007a, p. 379.

Keyvan-Ekbatani, M., A. Kouvelas, I. Papamichail, and M. Papageorgiou, Exploiting the fundamental diagram of urban networks for feedback-based gating. *Transportation Research Part B: Methodological*, Vol. 46, No. 10, 2012, pp. 1393–1403.

Doole, M., J. Ellerbroek, V. L. Knoop, and J. M. Hoekstra, Constrained Urban Airspace Design for Large-Scale Drone-Based Delivery Traffic. *Aerospace*, Vol. 8, No. 2, 2021, p. 38.

Cummings, C. and H. S. Mahmassani, Measuring the Impact of Airspace Restrictions on Air Traffic Flow Using Four-Dimensional System Fundamental Diagrams for Urban Air Mobility. *Transportation Research Record*, Vol. 2677, No. 1, 2023, pp. 1012–1026.

Aarts, M. J., J. Ellerbroek, and V. L. Knoop, Capacity of a constrained urban airspace: Influencing factors, analytical modelling and simulations. *Transportation Research Part C: Emerging Technologies*, Vol. 152, 2023, p. 104173.

Cummings, C. and H. Mahmassani, Emergence of 4-D System Fundamental Diagram in Urban Air Mobility Traffic Flow. *Transportation Research Record*, Vol. 2675, No. 11, 2021, pp. 841–850.

Tereshchenko, I., M. Hansen, and B. Zou, Macroscopic Fundamental Diagram for Air Traffic: Preliminary Theoretic Results and Simulation Findings. In *Proc., International Conference for Research in Air Transportation,(virtual)*, 2020.

Haddad, J., B. Mirkin, and K. Assor, Traffic flow modeling and feedback control for future Low-Altitude Air city Transport: An MFD-based approach. *Transportation Research Part C: Emerging Technologies*, Vol. 133, 2021, p. 103380.

Geroliminis, N. and C. F. Daganzo, Existence of urban-scale macroscopic fundamental diagrams: Some experimental findings. *Transportation Research Part B: Methodological*, Vol. 42, No. 9, 2008, pp. 759–770.

Edie, L., Discussion of traffic stream measurements and definitions. In *Proceedings of the Second International Symposium on the Theory of Traffic Flow*, OECD, Paris, France, 1965.

Administration, F. A., *JO 7210.3DD - Facility Operation and Administration – Traffic Management – National, Center, and Terminal Ground Delay Programs*, 2023.

Godfrey, J., The mechanism of a road network. *Traffic Engineering and Control*, Vol. 11, No. 7, 1969, pp. 323–327.

Mahmassani, H., J. C. Williams, and R. Herman, Investigation of network-level traffic flow relationships: some simulation results. *Transportation Research Record*, Vol. 971, 1984, pp. 121–130.

Daganzo, C., Urban gridlock: Macroscopic modeling and mitigation approaches. *Transportation Research Part B: Methodological*, Vol. 41, No. 1, 2007b, pp. 49–62.

Knoop, V. L. and S. P. Hoogendoorn, Empirics of a generalized macroscopic fundamental diagram for urban freeways. *Transportation Research Record*, Vol. 2391, No. 1, 2013, pp. 133–141.

Knoop, V. L., P. B. van Erp, L. Leclercq, and S. P. Hoogendoorn, Empirical MFDs using Google traffic data. In *2018 21st International Conference on Intelligent Transportation Systems (ITSC)*, IEEE, 2018, pp. 3832–3839.

Du, J., H. Rakha, and V. V. Gayah, Deriving macroscopic fundamental diagrams from probe data: Issues and proposed solutions. *Transportation Research Part C: Emerging Technologies*, Vol. 66, 2016, pp. 136–149.

Ambühl, L. and M. Menendez, Data fusion algorithm for macroscopic fundamental diagram estimation. *Transportation Research Part C: Emerging Technologies*, Vol. 71, 2016, pp. 184–197.

Loder, A., L. Ambühl, M. Menendez, and K. W. Axhausen, Understanding traffic capacity of urban networks. *Scientific reports*, Vol. 9, No. 1, 2019, pp. 1–10.

Gayah, V. V. and C. F. Daganzo, Clockwise hysteresis loops in the Macroscopic Fundamental Diagram: An effect of network instability. *Transportation Research Part B: Methodological*, Vol. 45, No. 4, 2011, pp. 643 – 655.

Hani Mahmassani, M. S. and A. Zockaie, Urban Network Gridlock: Characteristics, Dynamics and Control. In *Proceedings of the 20th International Symposium of Transporation and Traffic Theory*, 2013.

Cuniasse, P.-A., C. Buisson, J. Rodriguez, E. Teboul, and D. De Almeida, Analyzing railroad congestion in a dense urban network through the use of a road traffic network fundamental diagram concept. *Public Transport*, Vol. 7, No. 3, 2015, pp. 355–367.

Hoogendoorn, S. P., W. Daamen, V. L. Knoop, J. Steenbakkers, and M. Sarvi, Macroscopic fundamental diagram for pedestrian networks: theory and applications. *Transportation research procedia*, Vol. 23, 2017, pp. 480–496.

Johari, M., M. Keyvan-Ekbatani, L. Leclercq, D. Ngoduy, and H. S. Mahmassani, Macroscopic network-level traffic models: Bridging fifty years of development toward the next era. *Transportation Research Part C: Emerging Technologies*, Vol. 131, 2021, p. 103334.

Knoop, V. L., S. P. Hoogendoorn, and J. W. C. Van Lint, Routing Strategies Based on Macroscopic Fundamental Diagram. *Transportation Research Record: Journal of the Transportation Research Board*, Vol. 2315, No. 1, 2012, pp. 1–10.

Hajiahmadi, M., V. L. Knoop, B. De Schutter, and H. Hellendoorn, Optimal dynamic route guidance: A model predictive approach using the macroscopic fundamental diagram. In *16th international IEEE conference on intelligent transportation systems (ITSC 2013)*, IEEE, 2013, pp. 1022–1028.

Geroliminis, N., J. Haddad, and M. Ramezani, Optimal Perimeter Control for Two Urban Regions With Macroscopic Fundamental Diagrams: A Model Predictive Approach. *Intelligent Transportation Systems, IEEE Transactions on*, Vol. 14, No. 1, 2012, pp. 348–359.

Yuan, J., C. Wu, K. L. Teo, S. Zhao, and L. Meng, Perimeter Control With State-Dependent Delays: Optimal Control Model and Computational Method. *IEEE Transactions on Intelligent Transportation Systems*, 2022.

Daganzo, C., V. Gayah, and E. Gonzales, Macroscopic relations of urban traffic variables: Bifurcations, multivaluedness and instability. *Transportation Research Part B: Methodological*, Vol. 45, No. 1, 2011, pp. 278–288.

Schiphol Amsterdam airport, 2022, https://www.schiphol.nl/en/schiphol-group/page/transport-and-traffic-statistics/.

Ministerie van Infrastructuur en Milieu; Dutch Ministry of Infrastructure and Enviroment, *Luchtruimvisie (vision on the airspace, in Dutch)*. The Hague, 2012.

Knoop, V. L. and W. Daamen, Automatic fitting procedure for the fundamental diagram. *Transportmetrica B: Transport Dynamics*, Vol. 5, No. 2, 2017, pp. 129–144.

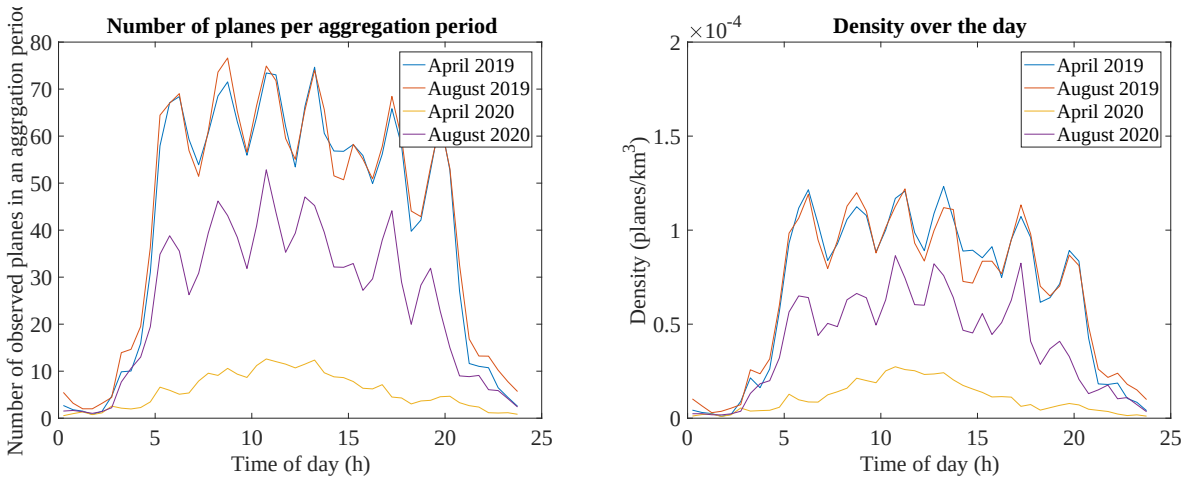

(a) Number of planes

(b) Density

Figure 2: The distribution of flights over the day

Figure 3: The considered area (CTA, blue line) and two flight trajectories into Schiphol

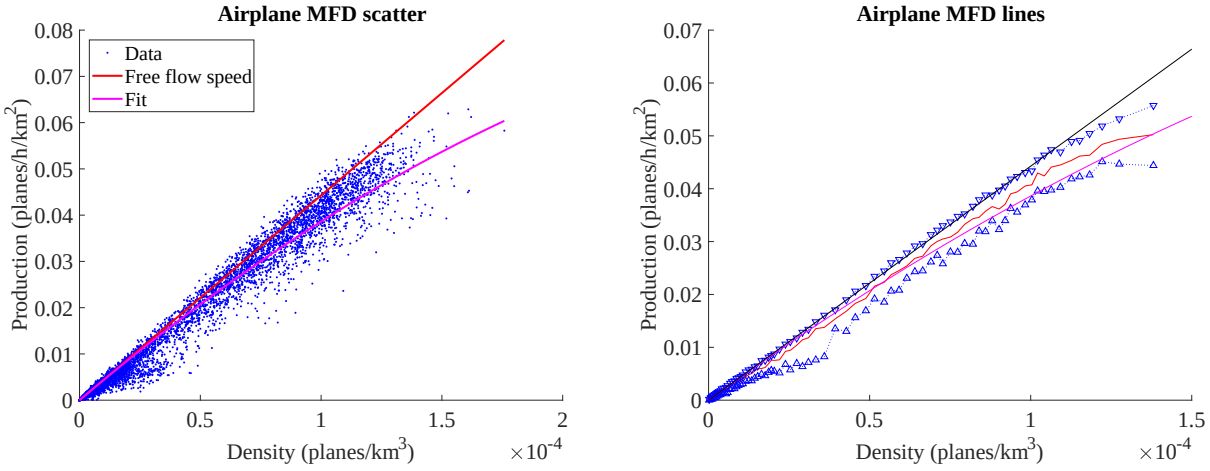

(a) scatter (b) trends

Figure 4: The MFD for airplanes.

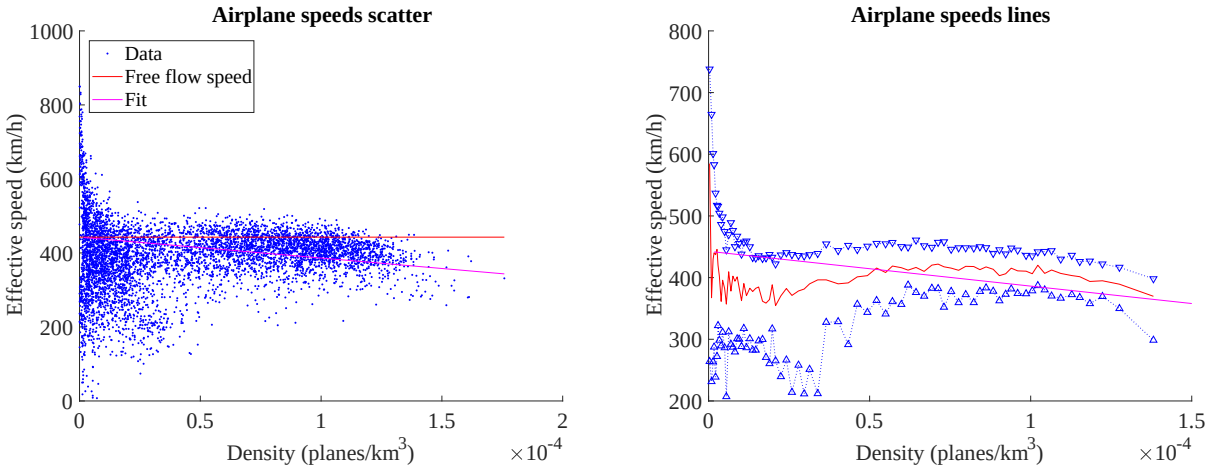

(a) scatter (b) trends

Figure 5: The effective speed of airplanes

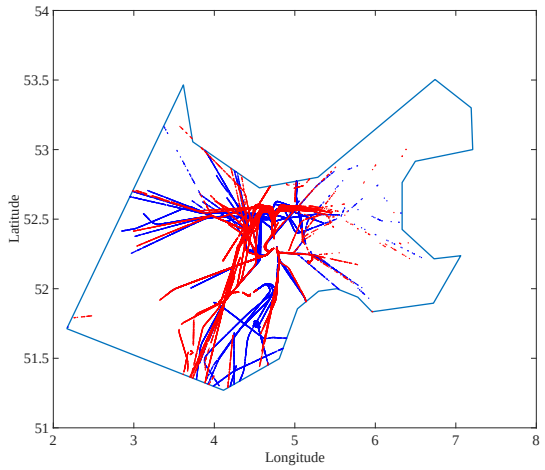

Figure 6: The routes of the plane during one busy hour (2 half hours each have a different color)

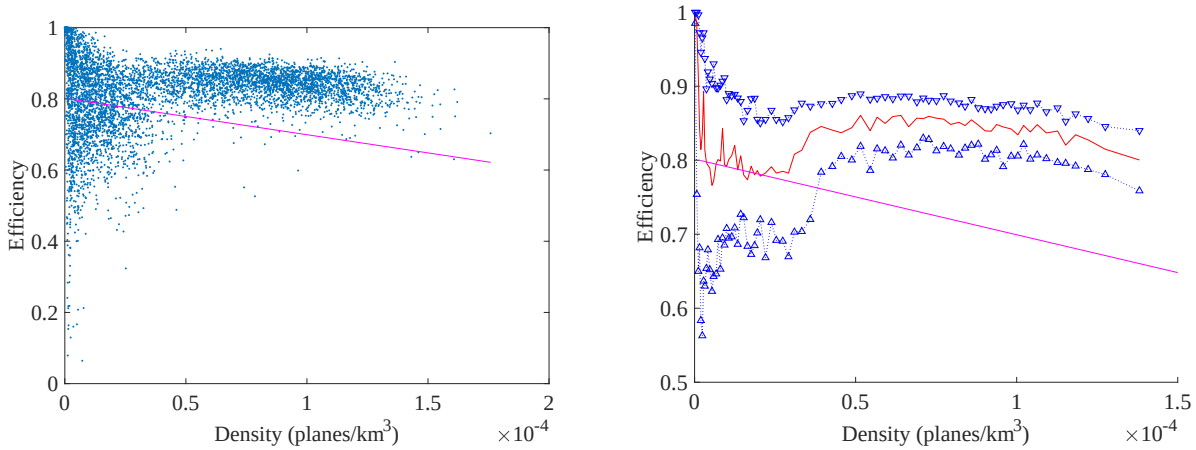

(a) Scatter (b) Line

Figure 7: The efficiency of the airspace